Xiangyu You, Junlei Duan, Keiichi Koda, Tatsuhiko Yamada and Yasumitsu Uraki*

Preparation of electric double layer capacitors (EDLCs) from two types of electrospun lignin fibers

DOI 10.1515/hf-2015-0175
Received August 5, 2015; accepted November 17, 2015; previously published online December 16, 2015

Abstract: Electrodes has been prepared for application in an electric double layer capacitor (EDLC) based on polyethylene glycol lignin (PEGL) and soda lignin (SL) derived from cedar wood. Fibers with a diameter of 23 μm were prepared by direct melt electrospinning of PEGL. Much finer fibers of 3.6 μm diameter were obtained by dry electrospinning of 70% PEGL in a dimethyl formamide (DMF) solution at 145°C. The dry electrospinning of SL alone in an alkaline aqueous solution was not achievable, but this was possible of a mixture of SL and polyethylene glycol (M_w=500 000) at a ratio of 99/1, which resulted in thin SL fibers with a diameter of 0.85 μm. These fibers were converted into activated carbon fibers (ACFs) by thermostabilization, carbonization, and steam activation. The specific Brunauer, Emmett and Teller (BET) surface areas of the resulting PEGL-ACFs and SL-ACFs were 1880 $m^2 g^{-1}$ and 1411 $m^2 g^{-1}$, respectively. PEGL-ACFs electrodes with an organic electrolyte exhibited an impedance of 1.6 Ω and a specific capacitance of 92.6 F g^{-1} at a scan rate of 1 A g^{-1}, and the SL-ACFs electrodes had an impedance and specific capacitance of 4.5 Ω and 55.6 F g^{-1}, respectively.

Keywords: activated carbon fibers, BET surface area, carbon fiber diameters, dry electrospinning, electric double layer capacitor, melt electrospinning, polyethylene glycol lignin, porosity, soda lignin, steam stabilization, thermostabilization

***Corresponding author: Yasumitsu Uraki,** Research Faculty of Agriculture, Hokkaido University, Sapporo, 060-8589, Japan, Phone: +81 011 706 2817, Fax: +81 011 706 2817, e-mail: uraki@for.agr.hokudai.ac.jp
Xiangyu You and Junlei Duan: Graduate School of Agriculture, Hokkaido University, Sapporo, 060-8589, Japan. http://orcid.org/0000-0001-9931-922X (X. You)
Keiichi Koda: Research Faculty of Agriculture, Hokkaido University, Sapporo, 060-8589, Japan
Tatsuhiko Yamada: Division of Biomass Chemistry, Forestry and Forest Products Research Institute, Tsukuba, 305-8687, Japan

Introduction

Lignin, a major component of wood, is a by-product of the pulping industry and it is primarily burned for energy recovery after concentration of the black liquor. Its use in other applications, such as dispersants (Aso et al. 2013), resins (Matsushita et al. 2006) and adhesives (Feldman 2002), has been investigated. However, only 2% of lignins (ca. 10^6 t y^{-1} of lignin sulfonates and $<10^5$ t y^{-1} of kraft lignins) are commercially utilized (Calvo-Flores and Dobado 2010). This is the reason why research activities are directed toward the development of high value-added materials from industrial lignins.

One of the current topics is to develop lignin based carbon materials, such as activated carbon and activated carbon fibers (ACFs) (Suzuki et al. 2008; Dobele et al. 2013; Huang and Zhao 2016). More recently, several papers described the preparation of electric double layer capacitor (EDLC) electrodes from lignin (Hu et al. 2014; Ruiz-Rosas et al. 2014; Zhang et al. 2014). You et al. (2015) also reported the preparation of electrodes from fine fibers of acetic acid lignin (AAL) for application in EDLCs. The electrostatic capacitance (C) is a relevant property of EDLCs, which depends on the surface area (A) of carbonaceous materials as one of the electrode components, and on the distance (d) between electrolyte ions and carbonaceous materials according to the following equation: $C=\varepsilon A/d$, where ε is the dielectric constant of the electrolyte (Chmiola et al. 2006). The strategy in our laboratory is the preparation of ACFs as carbonaceous materials with large surface areas. To this purpose, fine fibers have to be prepared by electrospinning in AAL/acetic acid solution; this dry electrospinning process is a well-known spinning method for obtaining fine fibers or nanofibers (Reneker and Chun 1996; Greiner and Wendorff 2007). In this process, the spinning molecules are highly charged and stretched by the electrostatic field. The fiber diameter is decreased during fiber formation due to electrostatic repulsion between the charged molecules (Huang et al. 2003). Fine AAL fibers with a diameter of 5.2 μm were obtained by dry electrospinning, and the fibers could be converted to ACFs with a Brunauer, Emmett and Teller (BET) specific surface area >2000 $m^2 g^{-1}$. Finally, EDLCs

was successfully assembled from ACFs and an organic electrolyte that had valuable electrochemical properties, including a specific capacitance of 133.3 F g^{-1} at a scan rate of 1 A g^{-1} and an energy density of 40 kW kg^{-1}.

In this study, the preparation of fine fibers was attempted by a new method of melt electrospinning, that combines melt spinning and electrospinning. Melt electrospun fibers can be expected to have advantages over conventional melt spun and dry electrospun fibers. The former produces thinner fibers than the latter, and it is more environmentally benign and less expensive because no solvent is needed in the preparation of the spinning dope. To achieve successful melt electrospinning, polyethylene glycol lignin (PEGL) was applied that was obtained by organosolv pulping of cedar wood with PEG 400 (Lin et al. 2012). PEGL was more thermally active with a lower glass transition temperature (T_g) and thermal flow-starting temperature (T_f) than AAL, which has been reported to be a fusible lignin (Uraki et al. 1995). In general, softwood lignins have lower thermal mobility than the corresponding hardwood lignins (Kubo et al. 1998).

The organosolv lignins AAL and PEGL are not commercially available. Thus, EDLC was assembled from soda lignin (SL) based ACF. Soda pulping has been well studied by the Forestry and Forest Products Research Institute, Tsukuba, Japan as a delignification process for bioethanol production based on cedar wood via enzymatic saccharification. Therefore, SL may be regarded as a commercially available technical lignin (Gosselink et al. 2004). However, cedar SL is not fusible; thus, SL was converted to fibers by dry electrospinning. Finally, PEGL and SL fine fibers were converted to ACFs, EDLCs and assembled with the resultant ACFs and an organic electrolyte, and their electrochemical performance was evaluated. The flow diagram of ACFs preparation and EDLC assembly is presented in Figure 1.

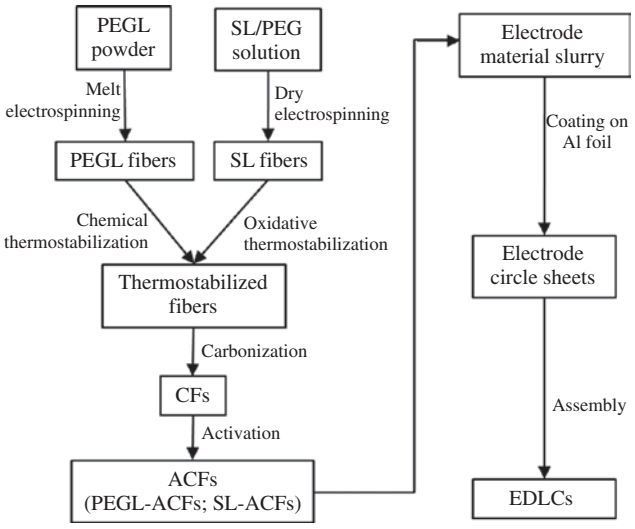

Figure 1: Flow diagram of ACFs preparation and EDLCs assembly.

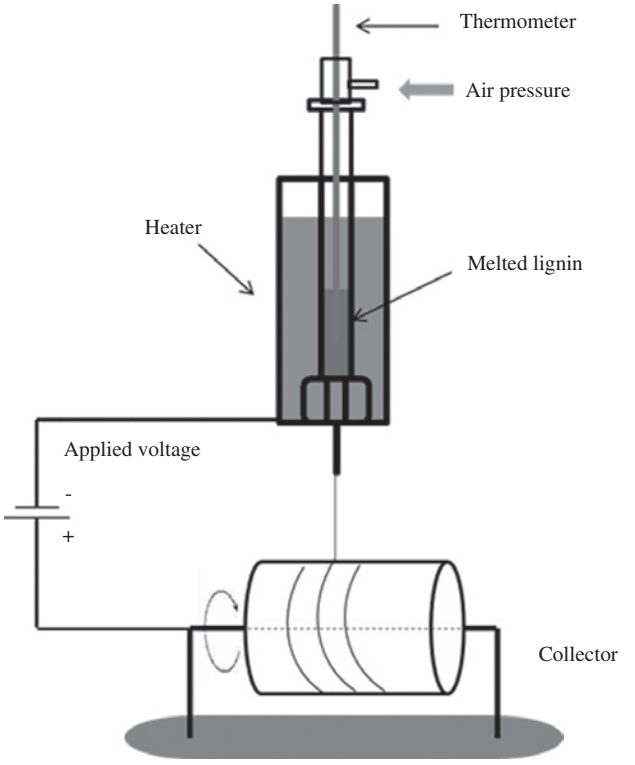

Figure 2: Schematic for the melt electrospinning setup.

Materials and methods

Lignin preparations: Cedar wood chips were subjected to soda pulping (Shibuya et al. 2015). The pulping conditions: pulping liquor was a 3.5% NaOH aqueous solution with 0.1% anthraquinone (b.o. dry weight); liquor-to-wood ratio of 5:1; heating time from room temperature (r.t.) to 170°C over 1.5 h and then maintained at 170°C for 3 h. The pulping was conducted in the Department of Biomass Chemistry, FFPRI (Tsukuba, Japan).

PEGL was isolated from cedar chips by organosolv pulping with PEG 400, which was purchased from Nacalai Tesque. Inc. (Kyoto, Japan) to obtain a PEGL powder according to Lin et al. (2012).

Melt electrospinning of PEGL: A melt electrospinning apparatus (Figure 2) was manufactured in the machinery laboratory of the Graduate School of Science, Hokkaido University. A spinneret is composed of a glass tube covered by a silicon-oil heater at the top and a metal needle as a nozzle (inside diameter, 0.8 mm) at the bottom. The distance between the nozzle and the rotary collector is 6 cm. An electrode from a high-voltage power supply is connected to the metal nozzle, and the fiber collector is connected to ground. PEGL powder was introduced into the glass tube, and the tube was then sealed and heated. When the temperature of the tube reached 175°C, a voltage of 20 kV was applied. The resulting fine fibers (spinning speed of

approximately 0.5 g h^{-1}) were collected on the rotary collector. Similarly, PEGL/dimethyl formamide (DMF) mixtures (70–90% by wt.) were electrospun by the same spinning apparatus at 145–150°C and a voltage of 20 kV.

Dry electrospinning of SL: SL alone and a mixture of SL and PEG 500 000 (Wako Pure Chemical Industries, Co., Ltd., Osaka, Japan) at SL/PEG ratios of 99/1 and 95/5 (w/w) were separately dissolved in DMF with stirring for 2.5 h at 80°C to prepare 35% solutions. The SL/DMF solution and the DMF solution of SL/PEG were subjected to dry electrospinning at r.t. under the following conditions: 25 kV; solution flow rate, 0.05 ml min^{-1}; and tip-collector distance, 13 cm.

Thermostabilization, carbonization and activation: Chemical thermostabilization of melt electrospun PEGL fibers was conducted as previously described (Lin et al. 2013). The PEGL fibers were immersed in 4 M or 6 M HCl for 1 or 2 h at 100°C and were then washed repeatedly with distilled water until the pH of the washings became 7. The treated fibers were dried in an oven at 105°C overnight. Afterwards, the fibers were heated to 250°C at a heating rate of 2°C min^{-1}, and the temperature was maintained for 1 h to obtain PEGL-based chemically thermostabilized fibers.

Electrospun SL fibers were produced by conventional oxidative thermostabilization. The SL fibers were directly heated without a chemical treatment to 250°C at a heating rate of 5°C min^{-1} and maintained at 250°C for 1 h to yield SL-based thermostabilized fibers.

Carbonization: The two types of thermostabilized fibers were carbonized under an N_2 stream at 1000°C for 1 h at a heating rate of 3°C min^{-1}. The resultant carbon fibers (CFs) were, in turn, transformed to ACFs by steam activation at 900°C for 1 h (heating rate, 10°C min^{-1}) under an N_2 stream at a flow rate of 0.5 l min^{-1}. For activation, 180 ml of water was dropped on a hot template at 150°C and a flow rate of 0.5 l h^{-1}, and the generated steam was introduced into the furnace with an N_2 stream. The fibers that were obtained from PEGL and SL are referred to as PEGL-ACFs and SL-ACFs, respectively.

EDLC assembly: EDLCs were assembled from the resultant ACFs and other additives as previously described (You et al. 2015). Briefly, SL-ACFs and PEGL-ACFs were ground together with conductive carbon black (CB, Super P conductive, 99+%, Alfa Aesar, Heysham, UK), and the mixtures were suspended in 2% aqueous sodium carboxymethyl cellulose (CMC, Wako Pure Chemical Industries, Co., Ltd., Osaka, Japan) solution. In the solution, the ratio of ACF:CMC:CB was 85:10:5 (b.o. dry weight). The mixture was then ultrasonicated for 2 h to yield a homogeneous slurry of electrode constituents. After this, Al foil (0.1 mm thick, 99.99% pure) was coated with the suspension and lignin-based electrodes were obtained by cutting the coated foil into 16 mm diameter circular sheets. The Al foil and a piece of paper (2 cm in diameter, 33 μm in thickness (Mitsubishi Paper Mills Ltd. (Tokyo, Japan) that served as a separator were immersed in an electrolyte solution (1.0 M triethylmethylammonium tetrafluoroborate ($TEAMBF_4$/PC) solution), and the air in the foil and sheet was removed under a vacuum for 3 h at r.t. One of the resultant Al foils was placed on the bottom of an electrode flat cell (Eager Corporation, Japan), and a cellulosic separator was placed on the foil. Afterwards, the other Al foil was placed on the separator. Finally, a steel plate, which was connected to the analyzer, was placed on the upper Al foil.

Instrumental analyses: Thermomechanical analysis (TMA) was conducted on a TMA-4000S System (MAC Science System 010, MAC Science, Yokohama, Japan) with a constant load of 5 g in a temperature range of 30–300°C under an N_2 flow of 0.15 l min^{-1}. The T_g and T_f were estimated from the first and second transition points in the TMA profiles, respectively (Kubo et al. 1996).

Fiber morphology was observed by an optical microscope (VK-9500 Violet Laser Color 3D profile microscope, Keyence Japan, Osaka, Japan), and a scanning electron microscope (SEM, JSM-6301F, JOEL Ltd., Tokyo, Japan) for gold-coated samples at an accelerating voltage of 5 kV.

N_2 adsorption/desorption isotherms were monitored at -196°C by means of a surface area analyzer (Autosorb-1, Quantachrome, Tokyo, Japan). The specific surface area was calculated from the N_2 adsorption isotherms in the relative pressure (P/P_0) range of 0.02–0.30 according to the BET model (Fitzer and Müller 1975; Sing, 1985). The total pore volume and the average pore size were calculated from adsorption isotherms based on the Quenched Solid Density Functional Theory (QSDFT) model (Neimark et al. 2009).

The electrochemical performance, specific capacitance, and impedance of the EDLCs were evaluated at an electrochemical workstation (Autolab PGSTAT302N FRA32M, Metrohm Autolab B.V., Tokyo, Japan). The specific capacitances were measured separately by cyclic voltammetry (CV) in a potential window of 0–3 V at a scan rate of 0.01-0.1 V s^{-1} and by galvanostatic charge/discharge (GCD) at a current density of 1 A g^{-1} according to equations 2 and 3 in the supplementary materials (Kim et al. 2013; You et al. 2015). The impedance was measured by electrochemical impedance spectroscopy (EIS) between 100 kHz and 10 mHz with an AC amplitude of 10 mV and the data were calculated from Nyquist plots.

PEG content was measured according to (Homma et al. 2008) approximately 0.2 g of a sample and 5 ml of HCl were mixed in a branched eggplant flask and then heated at 145°C for 90 min. All contents in the glass vessel were washed out with about 125 ml of 20% KI solution after cooling and then subjected to iodometric titration with 0.1 mol l^{-1} sodium thiosulfate solution. PEG content was calculated:

$$\mathrm{PEG\%}=[(V_s-V_b)/1000]\times 0.1\times(44/2)\times(1/W_s), \quad (1)$$

where V_s and V_b denote the titration volume of $Na_2S_2O_3$ for a sample and blank, respectively; W_s stands for the sample weight.

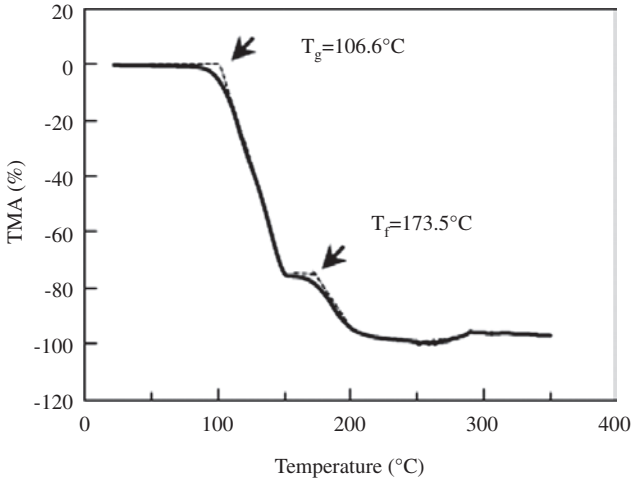

Figure 3: TMA of PEGL powder.

Cyclic voltammetry (CV) was monitored with a potential window from 0 to 3 V at different scan rates from 0.01 to 0.1 V s^{-1}, and specific capacitance was calculated from cyclic voltammogram according to (Qu and Shi 1998). Herein, $C_{1.5}$ (approximate value of real specific capacitance) at intermediate value in the potential range:

$$C_{1.5} = 4I/(mV/t), \tag{2}$$

where I is the current formed at the potential of 1.5 V, V/t is the potential scanning rate, and m refers to the total weight of the materials on two electrodes.

Galvanostatic charge/discharge (GCD) measurements were carried out at a current density of 1 A g^{-1} within the voltage range of 0–3 V. The specific capacitance, C, for a single electrode was calculated from the GCD curves (Qu and Shi 1998):

$$C = 4i(m\,dV/dt), \tag{3}$$

where i is the applied current, CMC and CB, and dV/dt is the slope obtained by fitting a straight line to the discharge curve over the range from 1.8 V to 1.35 V (60%–45% of V_{max}, where V_{max} is the maximum value of the operating potential window).

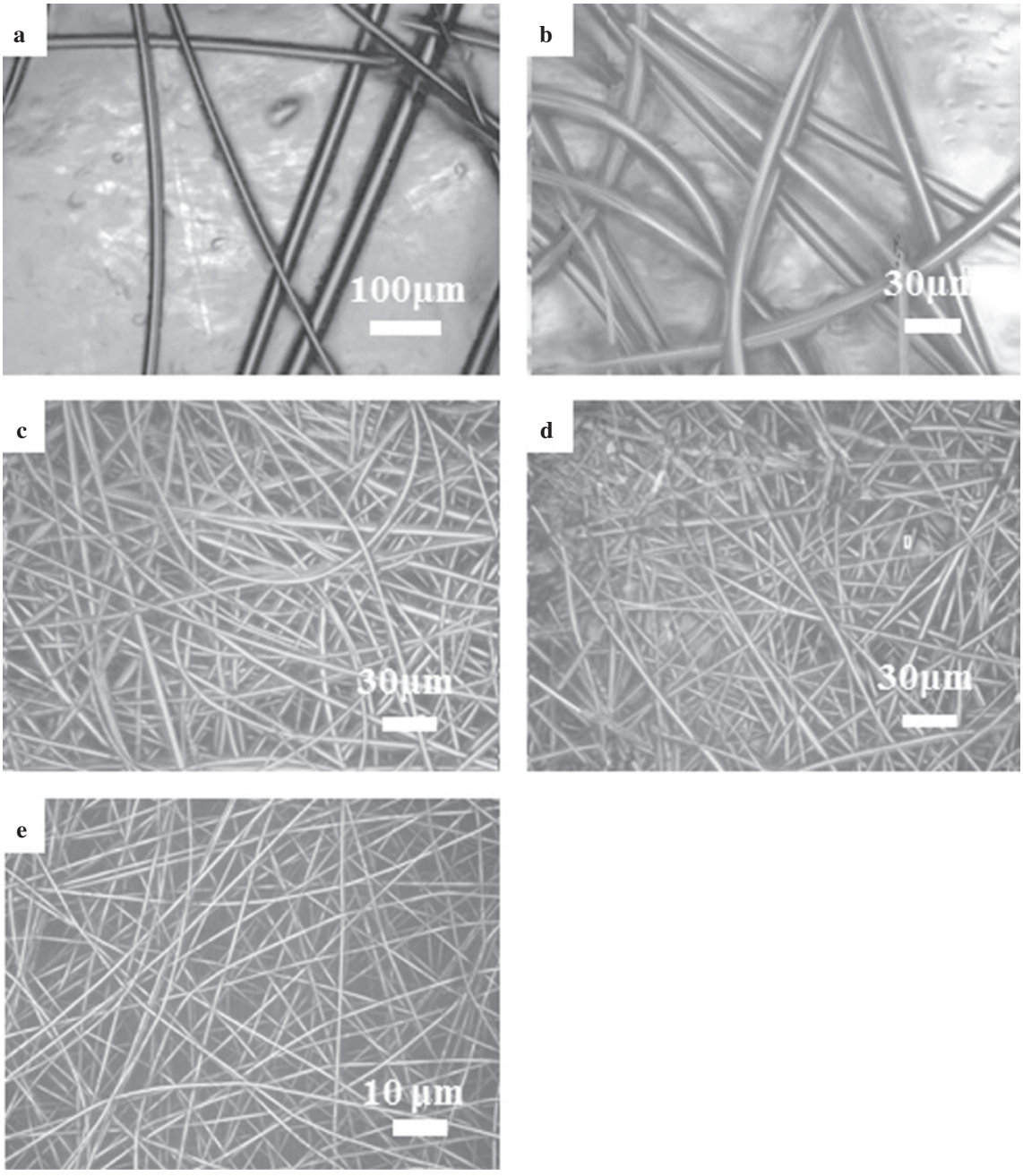

Figure 4: Images of melt electrospun PEGL fibers from (a) PEGL; PEGL/DMF at PEGL percentages of (b) 90%, (c) 80%, and (d) 70%; and (e) SL.

Results and discussion

Melt electrospinning of PEGL

A PEGL with a PEG content of 46.4% was obtained by organosolv pulping. The T_g and T_f of this PEGL were determined by TMA to evaluate the thermal properties. As shown in Figure 3, the TMA profile of PEGL displays two transition points at 106.6°C and 173.5°C, which correspond to the T_g and T_f, respectively (Kubo et al. 1996). These two transition temperatures are slightly lower than those of hardwood AAL, which has a T_g of 128°C and a T_f of 177°C (Uraki et al. 1995). Therefore, fusible PEGL is thermally more active than AAL. PEGL may be a more suitable material for melt electrospinning because it is less time and energy consuming.

PEGL was directly subjected to melt electrospinning. At a nozzle temperature of approx. 175°C and an applied

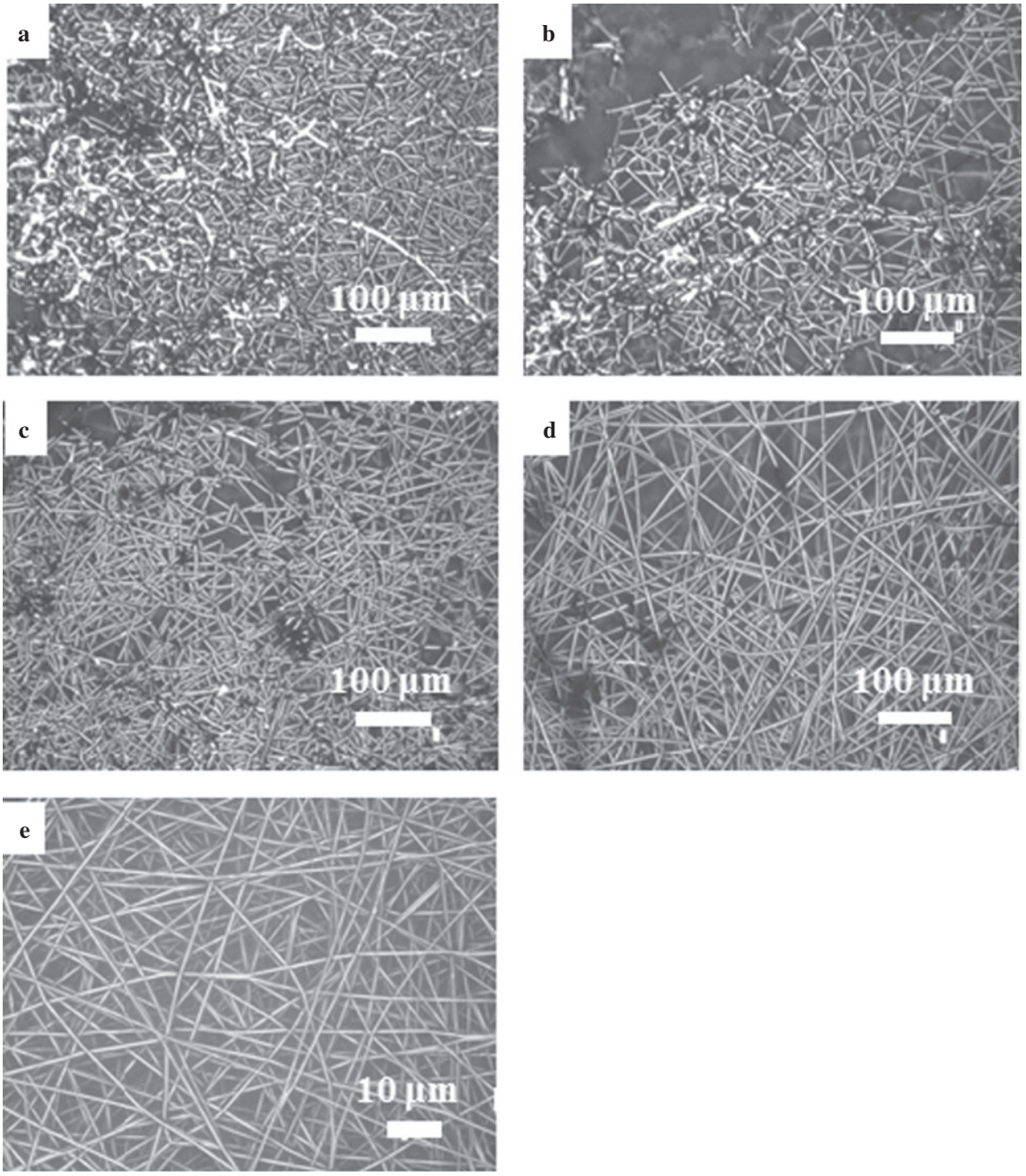

Figure 5: Images of melt electrospun fibers after chemical thermostabilization at a heating rate of 2°C min^{-1}: (a) PEGL; PEGL/DMF at PEGL percentages of (b) 90%, (c) 80%, and (d) 70%; and (e) SL.

voltage of 20 kV, PEGL was successfully melt electrospun into fibers (Figure 4a). The average diameter of the melt electrospun PEGL fibers was 18.0 μm, which is smaller than that of conventional melt spun PEGL fibers (23.0 μm) (Lin et al. 2012) but larger than that of AAL electrospun fibers (5.2 μm). To produce thinner fibers without changing the nozzle size, a small amount of solvent, DMF, was added to reduce the lignin concentration and the polymer viscosity.

PEGL/DMF mixtures at 70, 80 and 90% PEGL content were prepared and subjected to dry electrospinning in the same spinning apparatus as for melt electrospinning. The PEGL/DMF mixtures could be melt electrospun into fibers at a lower temperature (145–150°C) than could be done by PEGL alone. As shown in Figure 4b, thin fibers with a diameter of 7.6 μm could be obtained by the addition of 10% DMF. Increasing the DMF content to 20% led to a decrease in the fiber diameter to 3.5 μm, and the thinnest fibers, with a diameter of 3.2 μm, were obtained with 30% DMF. No heating the spinneret produced conditions that mimic the normal dry electrospinning of the solution, and fibers could not be obtained from these highly concentrated PEGL/DMF solutions. Compared with conventional dry electrospinning, melt electrospinning not only remarkably decreases the diameter of the fibers but also reduces the amount of solvent and lowers the spinning temperature, thereby decreasing the cost of the production process.

Dry electrospinning of SL

Dry electrospinning of SL alone in DMF was incapable for producing fine fibers because droplets formed on the collector. Hence, dry electrospinning of a mixture of SL and PEG was attempted because the addition of high molecular weight polyethylene oxide (M_w=10^6 g mol^{-1}) was reported to improve the spinnability of lignin (Dallmeyer et al. 2010). A mixture of SL and PEG 500 000 at a ratio of 99/1 in DMF (35%) could be electrospun into thin fibers with an average diameter of 0.85 μm (Figure 4e). However, when the content of PEG 500 000 was increased, the solution could not be spun constantly because of its high viscosity.

Thermostabilization of PEGL and SL fibers

As shown in Figure 5, PEGL fibers treated with 4 M HCl at 100°C for 1 and 2 h both melted. In contrast, fibers treated with 6 M HCl at 100°C for 1 h partially melted. When the treatment time was increased to 2 h, the resultant fibers became infusible. This was attributed to the release of PEG moieties from the PEGL by acid hydrolysis (Lin et al. 2012), which resulted in suppression of the thermal mobility of PEGL fibers.

The TMA profiles of the resultant fibers (Figure 6) also supported the results of the visual inspection of fusibility. Before chemical thermostabilization, the fibers had a T_g of 119.2°C and a T_f of 182.8°C (Figure 6a). Noticeably, after chemical thermostabilization (6 M HCl at 100°C for 2 h and thermal treatment in air at 250°C for 1 h, for a total of 3 h), the T_f was eliminated from the TMA profile, and the T_g was significantly increased to 190.2°C (Figure 6b). Thus, the thermal mobility of the PEGL fibers was dramatically suppressed by chemical thermostabilization. The entire process for the conversion to infusible fibers was completed in 5 h, and this short treatment time contributes to the time and energy savings.

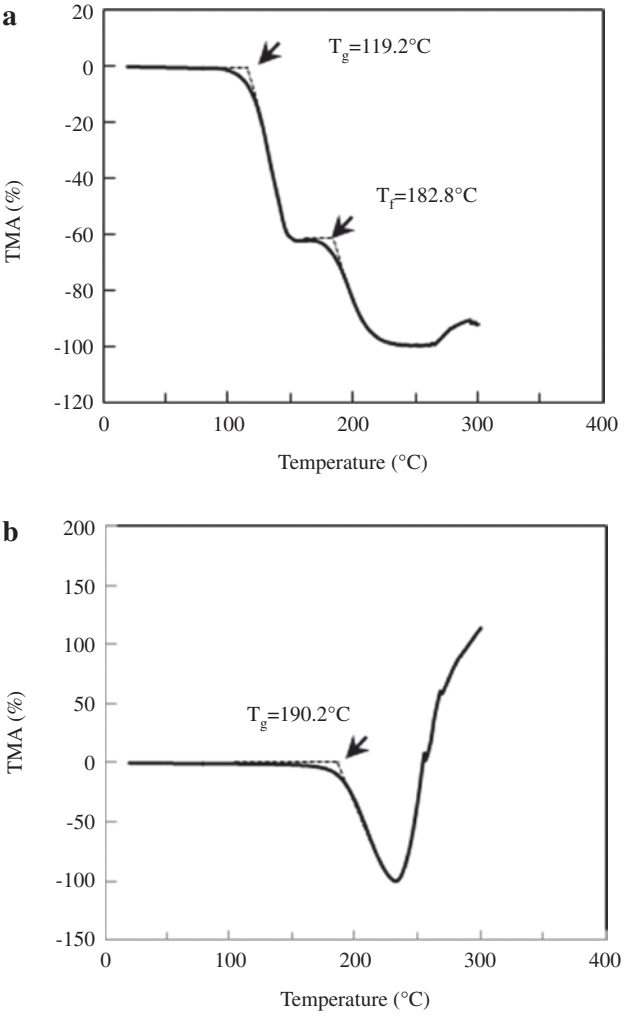

Figure 6: TMA of 70% PEGL/DMF fibers before (a) and after (b) chemical thermostabilization.

As shown in Figure 5e, SL fibers could be thermostabilized by a heating rate of 5°C min^{-1} for a conventional oxidative treatment with air. The heating rate was comparable to the highest heating rate previously reported, which was carried out with kraft lignin (Dallmeyer et al. 2014). The simple conversion of SL to an infusible form can be attributed to the low thermal mobility of the original SL, which is attributed to its highly condensed structure.

Preparation of ACFs by carbonization and activation

To prepare CFs, the thermostabilized fibers were subjected to carbonization. The SEM images in Figure 7a demonstrate that that the resultant PEGL-CFs maintained their fiber morphology with a diameter of 2.6 μm and that defects were observable on the fiber surface; these defects were likely caused by the HCl treatment during chemical thermostabilization and the thermal removal of a portion of the residual PEG moieties from the fibers (Lin et al. 2012). SL-CFs with a diameter of 0.7 μm were obtained from the thermostabilized fibers, as shown in Figure 7b. In contrast to the defects that were observed in the PEGL-CFs surface, SL-CFs exhibited more distinctive pores in the surface, indicating that the SL fibers were more easily removed during thermal carbonization.

Figure 7c and d depict the morphology of the resultant PEGL- and SL-ACFs, respectively. Steam activation caused the fiber diameter of the PEGL-ACFs to decrease to 1.9 μm. In contrast, SL-ACFs had a much smaller fiber diameter of 270 nm (nanofiber level) and a more porous structure on the surface and the inside of the fibers.

Surface area and porosity of ACFs

The BET specific surface area and porosity parameters, along with the pore volumes and average pore diameters, are listed in Table 1. PEGL-CFs had a large BET surface area of 1114 $m^2 g^{-1}$, whereas SL-CFs had a smaller value of 635 $m^2 g^{-1}$. Both CFs were converted to ACFs under the same activation conditions with 180 ml at 1000°C. The BET

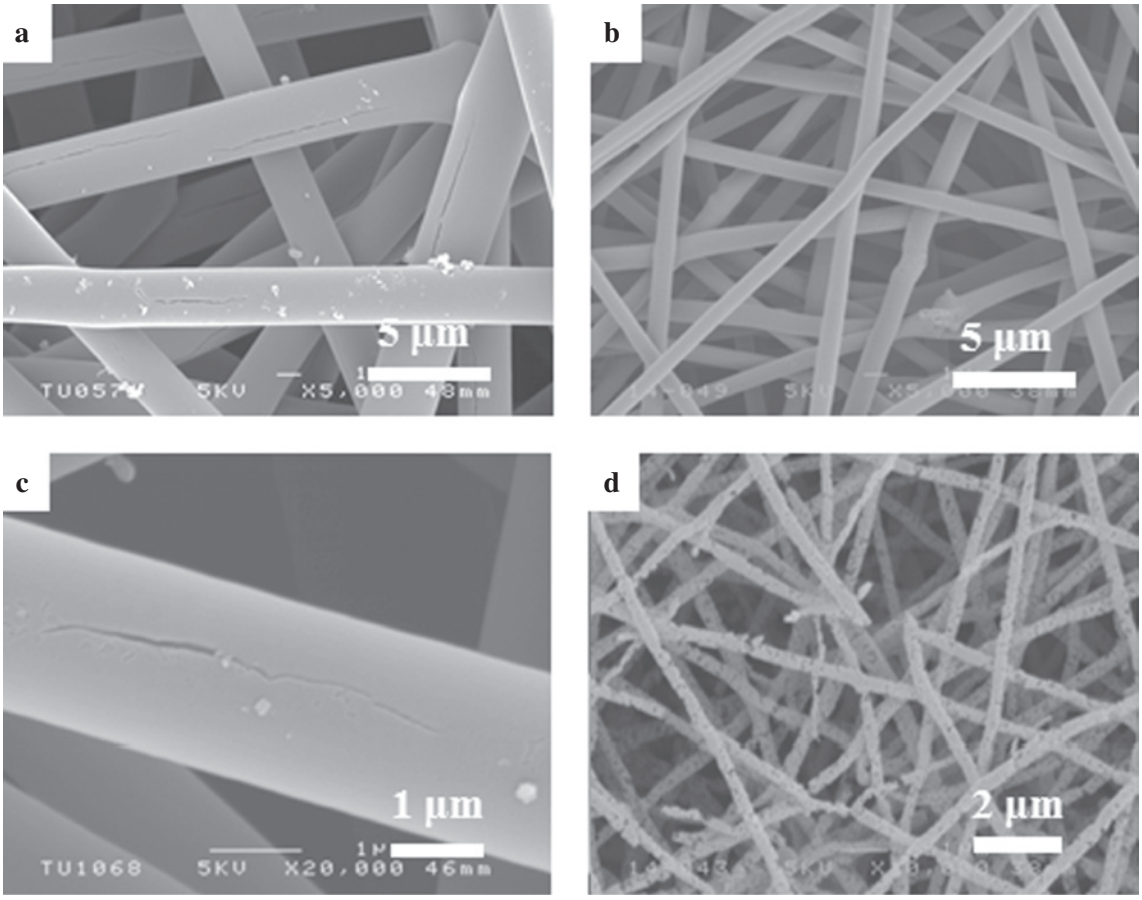

Figure 7: Images of CFs and ACFs: (a) PEGL-CFs; (b) SL-CFs; (c) PEGL-ACFs; and (d) SL-ACFs.

Table 1: Surface area and pore parameters of carbonaceous materials and the properties of the assembled EDLC.

Sample	Activation yield (%)	Specific surface area ($m^2 g^{-1}$)[a]	Total pore volume ($ml g^{-1}$)[b]	Avrg. pore diam. (nm)[b]	Specific capacitance ($F g^{-1}$)[c]	Intrinsic resistance (Ω)
PEGL-CFs	–	1114	0.48	0.90	–	–
SL-CFs	–	635	0.47	2.97	–	–
PEGL-ACFs	41.8	1880	0.83	0.91	92.6	1.6
SL-ACFs	70.0	1411	1.67	4.73	55.6	4.5

Calculated by the [a]BET model, [b]QSDFT model, and the [c]GCD method.

surface area of the PEGL-ACFs was increased to 1880 $m^2 g^{-1}$ with an average pore diameter of 0.91 nm. In contrast, the BET surface area of the SL-ACFs was only 1411 $m^2 g^{-1}$. In addition, its average pore diameter of 4.73 nm was much larger than that of the PEGL-ACFs. It has been reported that the difference in the BET surface area and the pore diameter of PEGL-ACFs and SL-ACFs affects the electric performance of the EDLCs (Chmiola et al. 2006).

Electrochemical properties

The electrochemical performances of $EDLC_{PEGL\text{-}ACFs}$ and $EDLC_{SL\text{-}ACFs}$ were evaluated by CV, GCD and EIS. CV measurements were conducted at three different scanning rates of 0.01, 0.05 and 0.1 V s^{-1} between 0 and 3.0 V. The obtained CV curves are presented in Figure 8. All of the CV curves for the $EDLC_{PEGL\text{-}ACFs}$ exhibited an approximately rectangular shape at the three scanning rates (Figure 8a); this shape is similar to a typical CV profile for EDLCs with stable performance, as previously reported (Wang et al. 2012), indicating that the electric double layer was well-formed. According to equations (2) and (3), the specific capacitances at the scan rates of 0.01, 0.05 and 0.1 V s^{-1} were calculated to be 67.0, 69.7 and 67.1 F g^{-1}, respectively. Regarding the $EDLC_{SL\text{-}ACFs}$, all of the CV curves obtained at all scan rates also showed the typical rectangular shape (Figure 8b), suggesting the adequate formation of an electric double layer. At scan rates of 0.01, 0.05 and 0.1 V s^{-1}, the specific capacitances were calculated to be 57.5, 53.2 and 54.2 F g^{-1}, respectively.

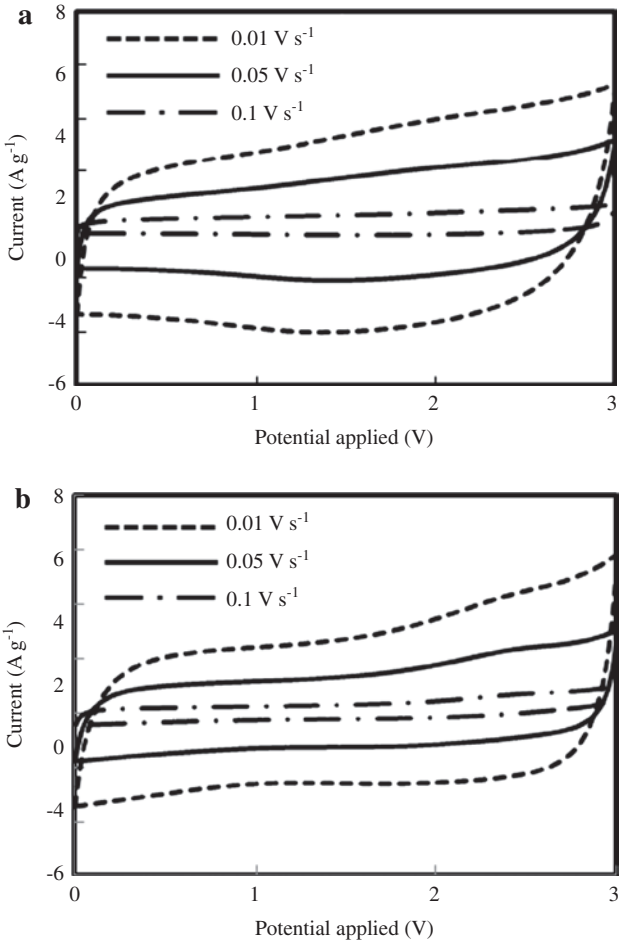

Figure 8: CV of (a) PEGL-ACFs and (b) SL-ACFs based EDLCs at different scan rates.

Figure 9 shows GCD profiles of $EDLC_{PEGL\text{-}ACFs}$ and $EDLC_{SL\text{-}ACFs}$ at a current density of 1 A g^{-1}. Compared with $EDLC_{SL\text{-}ACFs}$, the $EDLC_{PEGL\text{-}ACFs}$ had a longer discharge time, indicating a larger capacitance for the $EDLC_{PEGL\text{-}ACFs}$ (Figure 9a). In addition, the isosceles triangular shape of the profile indicated good charge/discharge performance for the $EDLC_{PEGL\text{-}ACFs}$. In contrast, $EDLC_{SL\text{-}ACFs}$ exhibited a slightly asymmetrical triangular shape (Figure 9b), indicating a relatively low charge–discharge efficiency compared with $EDLC_{PEGL\text{-}ACFs}$. Accordingly, $EDLC_{PEGL\text{-}ACFs}$ had a larger specific capacitance of 92.6 F g^{-1} at 1 A g^{-1} than $EDLC_{SL\text{-}ACFs}$ (55.6 F g^{-1}).

EIS is a semi-quantitative method for determining the impedance of EDLCs. In this study, a Nyquist plot was employed to characterize the EIS spectra. The intrinsic resistance of an EDLC is the sum of the intrinsic resistances of the electrolyte and the ACFs and of the contact resistance between the ACFs and the current collector,

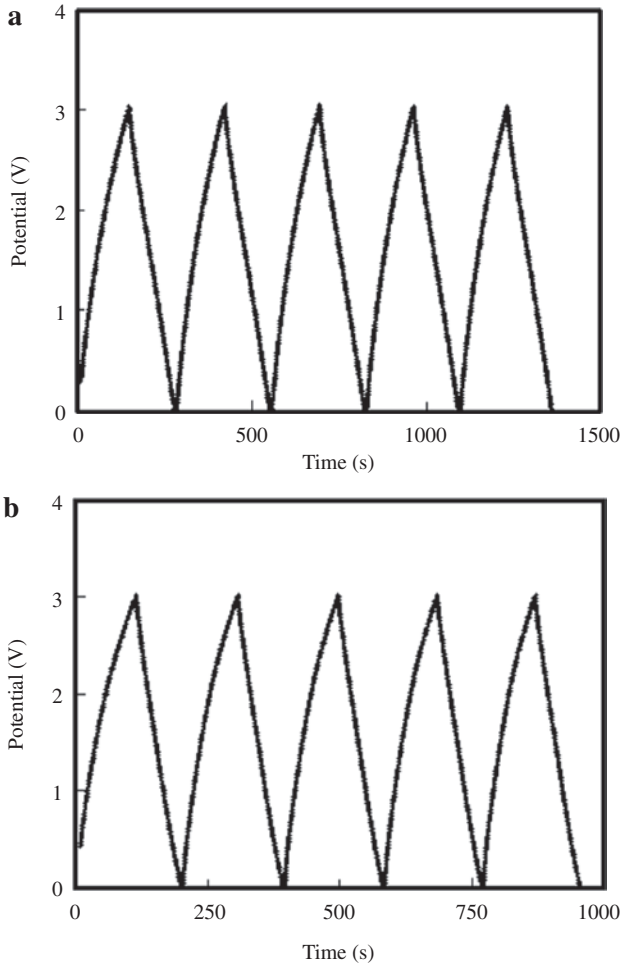

Figure 9: GCD profiles of EDLCs based on (a) PEGL-ACFs and (b) SL-ACFs for a current density of 1 A g^{-1}.

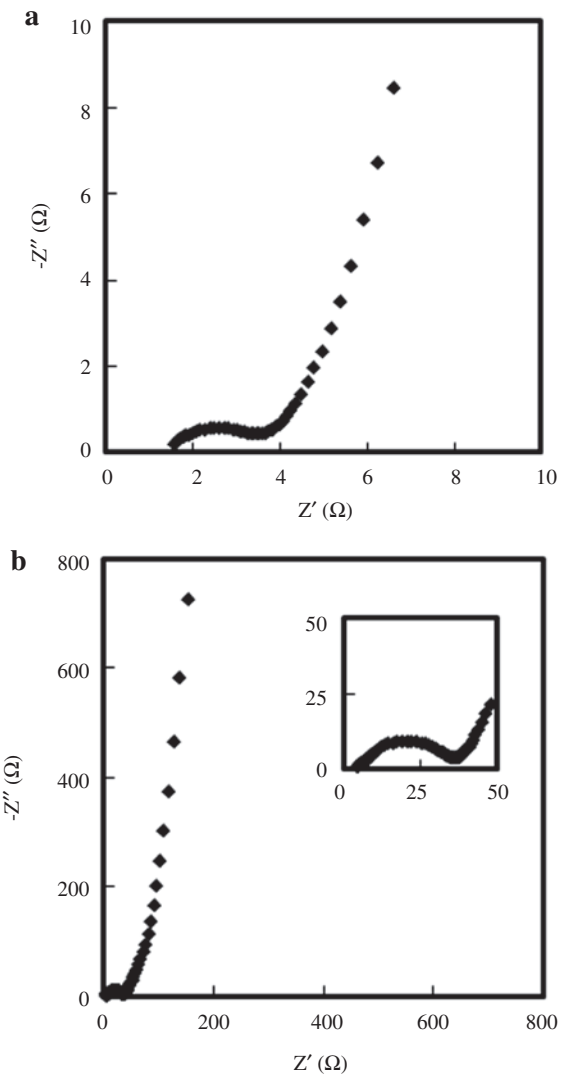

Figure 10: Nyquist plots of EDLCs based on (a) PEGL-ACFs and (b) SL-ACFs. The inset is a magnification of the high-frequency region.

and the intrinsic resistance is obtained at the intercept on the *Z'* axis in Nyquist plots (Liu et al. 2008; Liu et al. 2012). $EDLC_{PEGL\text{-}ACFs}$ possess a lower intrinsic resistance (1.6 Ω) than $EDLC_{SL\text{-}ACFs}$ (4.5 Ω) (Table 1). Polarization resistance, which is another resistance parameter for evaluating the electrolyte mobility for the adsorption and desorption rates of the electrolyte onto/from the pores of a carbonaceous electrode, could also be estimated from the length or diameter of the semi-circle in a high-frequency region of the Nyquist plot, as shown in the Figure 10a and b (Liu et al. 2008). $EDLC_{PEGL\text{-}ACFs}$ clearly exhibit a shorter arc (2.1 Ω) than $EDLC_{SL\text{-}ACFs}$ (33.5 Ω).

This inferior performance of $EDLC_{SL\text{-}ACFs}$ was attributed to the smaller BET surface area and the larger pore size of SL-ACFs compared with that of PEGL-ACFs (Chmiola et al. 2006). A carbonaceous material with a larger surface area can contain more electrolyte ions. In addition, the adsorption of electrolyte ions on the smaller pores of the material facilitates the contact between the ions and the material. As a result, carbonaceous materials with large surface areas and small pore diameters have a large capacitance and low impedance.

Conclusions

Thin lignin fibers were successfully prepared from thermally fusible PEGL and infusible SL. Although PEGL fibers could be spun by melt electrospinning, much finer fibers could be obtained in the same spinning apparatus by the addition of a small amount of DMF. Dry electrospinning of SL and PEG mixtures could also give rise to thin fibers, although only 1% PEG was added. In addition, these thin PEGL and SL fibers were both readily converted to

thermostabilized fibers through a high heating rate, which resulted in time and energy savings with this treatment.

The resultant PEGL-ACFs had a larger BET surface area and a smaller pore diameter than SL-ACFs. Compared with $EDLC_{SL\text{-}ACFs}$, the assembled $EDLC_{PEGL\text{-}ACFs}$ had a larger specific capacitance and a lower intrinsic impedance. The superior performance of the $EDLC_{PEGL\text{-}ACFs}$ was attributed to their large BET surface area and small average pore diameter. Taking into consideration the excellent performance of $EDLC_{AAL\text{-}ACFs}$, the organosolv lignins (PEGL and AAL) were better suited as feedstocks than alkali lignins (SL) as an electrode material for assembling EDLCs. It was expected that the pulping solvent could introduce PEG 400 and acetic acid into PEGL and AAL molecules, respectively, which could then be burned off to form small pores on the fiber surface to allow the accumulation of electrolyte ions.

Acknowledgments: This work was supported by a grant from the Ministry of Agriculture, Forestry and Fisheries of Japan, "Development of Technologies for Biofuel Production Systems in Rural Areas (2012–2015)".

References

Aso, T., Koda, K., Kubo, S., Yamada, T., Nakajima, I., Uraki, Y. (2013) Preparation of novel lignin-based cement dispersants from isolated lignins. J. Wood Chem. Technol. 33:286–298.

Calvo-Flores, F.G., Dobado, J.A. (2010) Lignin as renewable raw material. ChemSusChem 3:1227–1235.

Chmiola, J., Yushin, G., Gogotsi, Y., Portet, C., Simon, P., Taberna, P.L. (2006) Anomalous increase in carbon capacitance at pore sizes less than 1 nanometer. Sci. 313:1760–1763.

Dallmeyer, I., Ko, F., Kadla, J.F. (2010) Electrospinning of technical lignins for the production of fibrous networks. J. Wood Chem. Technol. 30:315–329.

Dallmeyer, I., Lin, L.T., Li, Y., Ko, F., Kadla, J.F. (2014) Preparation and characterization of interconnected, kraft lignin-based carbon fibrous materials by electrospinning. Macromol. Mater. Eng. 299:540–551.

Dobele, G., Vervikishko, D., Volperts, A., Bogdanovich, N., Shkolnikov, E. (2013) Characterization of the pore structure of nanoporous activated carbons produced from wood waste. Holzforschung 67:587–594.

Feldman, D. (2002) Lignin and its polyblends – a review. In: Chemical Modification, Properties, and Usage of Lignin. Ed. Hu, T. Springer, US. pp.81–99.

Fitzer, E., Müller, D.J. (1975) The influence of oxygen on the chemical reactions during stabilization of pan as carbon fiber precursor. Carbon 13:63–69.

Gosselink, R., De Jong, E., Guran, B., Abächerli, A. (2004) Co-ordination network for lignin – standardisation, production and applications adapted to market requirements (EUROLIGNIN). Ind. Crops Prod. 20:121–129.

Greiner, A., Wendorff, J.H. (2007) Electrospinning: a fascinating method for the preparation of ultrathin fibers. Angew. Chem. Int. Ed. 46:5670–5703.

Homma, H., Kubo, S., Yamada, T., Matsushita, Y., Uraki, Y. (2008) Preparation and characterization of amphiphilic lignin derivatives as surfactants. J. Wood Chem. Technol. 28:270–282.

Hu, S., Zhang, S., Pan, N., Hsieh, Y.-L. (2014) High energy density supercapacitors from lignin derived submicron activated carbon fibers in aqueous electrolytes. J. Power Sources 270:106–112.

Huang, Y., Zhao, G. (2016) Preparation and characterization of activated carbon fibers from liquefied wood by KOH activation. Holzforschung 70:195–202.

Huang, Z.-M., Zhang, Y.-Z., Kotaki, M., Ramakrishna, S. (2003) A review on polymer nanofibers by electrospinning and their applications in nanocomposites. Compos. Sci. Technol. 63:2223–2253.

Kim, T., Jung, G., Yoo, S., Suh, K.S., Ruoff, R.S. (2013) Activated graphene-based carbons as supercapacitor electrodes with macro- and mesopores. ACS Nano 7:6899–6905.

Kubo, S., Uraki, Y., Sano, Y. (1996) Thermomechanical analysis of isolated lignins. Holzforschung 50:144–145.

Kubo, S., Uraki, Y., Sano, Y. (1998) Preparation of carbon fibers from softwood lignin by atmospheric acetic acid pulping. Carbon 36:1119–1124.

Lin, J., Kubo, S., Yamada, T., Koda, K., Uraki, Y. (2012) Chemical thermostabilization for the preparation of carbon fibers from softwood lignin. BioResources 7:5634–4646.

Lin, J., Koda, K., Kubo, S., Yamada, T., Enoki, M., Uraki, Y. (2013) Improvement of mechanical properties of softwood lignin-based carbon fibers. J. Wood Chem. Technol. 34:111–121.

Liu, C.L., Dong, W.S., Cao, G.P., Song, J.R., Liu, L., Yang, Y.S. (2008) Capacitance limits of activated carbon fiber electrodes in aqueous electrolyte. J. Electrochem. Soc. 155:F1–F7.

Liu, S., Song, Y., Ma, C., Shi, J.-l., Guo, Q.-g., Liu, L. (2012) The electrochemical performance of porous carbon nanofibers produced by electrospinning. Carbon 50:3963.

Matsushita, Y., Wada, S., Fukushima, K., Yasuda, S. (2006) Surface characteristics of phenol-formaldehyde-lignin resin determined by contact angle measurement and inverse gas chromatography. Ind. Crops Prod. 23:115–121.

Neimark, A.V., Lin, Y., Ravikovitch, P.I., Thommes, M. (2009) Quenched solid density functional theory and pore size analysis of micro-mesoporous carbons. Carbon 47:1617–1628.

Qu, D., Shi, H. (1998) Studies of activated carbons used in double-layer capacitors. J. Power Sources 74:99–107.

Reneker, D.H., Chun, I. (1996) Nanometre diameter fibres of polymer, produced by electrospinning. Nanotechnology 7:216.

Ruiz-Rosas, R., Valero-Romero, M.J., Salinas-Torres, D., Rodríguez-Mirasol, J., Cordero, T., Morallón, E., Cazorla-Amorós, D. (2014) Electrochemical performance of hierarchical porous carbon materials obtained from the infiltration of lignin into zeolite templates. ChemSusChem 7:1458–1467.

Shibuya, H., Magara, K., Nojiri, M. (2015) Cellulase production by Trichoderma reesei in fed-batch cultivation on soda-anthraquinone pulp of the Japanese cedar. Bulletin of FFPRI 14:29–35.

Sing, K.S.W. (1985) Reporting physisorption data for gas/solid systems with special reference to the determination of surface area and porosity (Recommendations 1984). Pure Appl. Chem. 57:603–619.

Suzuki, K., Suzuki, T., Takazawa, N., Funaoka, M. (2008) Crystallinity and mesoporosity of carbon produced from ligno-p-cresol and their improvement by pulverization and acid treatment. Holzforschung 62:157–163.

Uraki, Y., Kubo, S., Nigo, N., Sano, Y., Sasaya, T. (1995) Preparation of carbon fibers from organosolv lignin obtained by aqueous acetic acid pulping. Holzforschung 49:343–350.

Wang, G., Zhang, L., Zhang, J. (2012) A review of electrode materials for electrochemical supercapacitors. Chem. Soc. Rev. 41:797–828.

You, X., Koda, K., Yamada, T., Uraki, Y. (2015) Preparation of electrode for electric double layer capacitor from electrospun lignin fibers. Holzforschung 69:1097–1106.

Zhang, F., Lu, Y.H., Yang, X., Zhang, L., Zhang, T.F., Leng, K., Wu, Y.P., Huang, Y., Ma, Y.F., Chen, Y.S. (2014) A flexible and high-voltage internal tandem supercapacitor based on graphene-based porous materials with ultrahigh energy density. Small 10:2285–2292.